Journal of the European Ceramic Society 21 (2001) 409–417

www.elsevier.com/locate/jeurceramsoc

A microstructural study of porous piezoelectric ceramics obtained by different methods

E. Roncari [a,*], C. Galassi [a], F. Craciun [b], C. Capiani [a], A. Piancastelli [a]

[a] *CNR Istituto di Ricerche Tecnologiche per la Ceramica, via Granarolo 64, I-48018, Faenza, Italy*
[b] *CNR Istituto di Acustica, Area di Ricerca Roma-Tor Vergata, via del Fosso del Cavaliere 100, I-00133, Rome, Italy*

Received 25 May 2000; accepted 9 July 2000

Abstract

Piezoelectric porous lead zirconate titanate (PZT) ceramics prepared by different methods have been examined from a microstructural point of view. The effect of polymer volume and properties and sintering temperature on microstructure of samples and on their physical properties has been investigated. The wide range of pore volumes and pore size distributions was obtained by three different procedures: (a) reduction of the sintering temperature of the die pressed PZT samples; (b) use of a different forming technique like tape casting, starting from slurries with high volume of organic content; (c) addition of different volume concentrations of organic polymer to the PZT powder. It has been found that varying process parameters like quantity of polymer and sintering temperature changes both final porosity as well as pore size distribution, introducing dispersion in physical property values. The differences between the microstructural aspect of samples prepared by different methods and their influence on the physical properties of the samples are presented and discussed.

Keywords: Microstructure-final; Piezoelectric properties; Porosity; PZT; Sintering

1. Introduction

Piezoelectric materials have been widely studied for the possibility they give to convert electrical signals to mechanical signals and viceversa. They have been largely used in ultrasonic transducers for passive and active applications like hydrophones, sensors, actuators, biomedical imaging etc. Porous piezoelectric ceramics have been developed due to the possibility of obtaining very high values for some piezoelectric coefficients with respect to dense materials.[1–12] Moreover other limitations of dense piezoceramic materials, regarding poor acoustic matching between the ceramic and the media through which it is transmitting or receiving a signal, are solved by these materials where air inclusions decrease the effective acoustical impedance.[10] It has been shown that they can be successfully employed in different applications like transducers for medical ultrasonic imaging[4] and hydrophones.[7,8,13] In the vicinity of percolation threshold,[14] porous ceramics behave like self-similar percolating systems, with physical properties following scaling power laws.[9,15–17] Therefore some piezoelectric coefficients could be highly increased in very porous systems.[9,18] Nevertheless in many useful systems one should make a compromise between increasing of those properties and maintaining a good mechanical resistance, therefore choosing somewhat lower porosities regime. In previous studies we have noted that far from percolation, when one plots properties as a function of porosity, there is a dispersion in the results of properties of ceramics, which should originate from microstructural differences.[10] Moreover, similar differences can be observed between samples prepared by different methods, as reported in other papers.[3,5,10,12]

The techniques most commonly used to obtain porous ceramics are the polymer foam impregnation and the foaming method while other techniques focus on the ceramic powder compounding and sintering (particle size distribution),[19] fugitive organic compounds addi-

* Corresponding author. Tel.: +39-546-699753; fax: +39-546-46381.
E-mail address: roncari@irtec1.irtec.bo.cnr.it (E. Roncari).

0955-2219/01/$ - see front matter
PII: S0955-2219(00)00208-9

tion[20] and/or particle interactions in the powder suspensions prior to the forming operation.[21] In the first case, a polymer sponge is soaked in the ceramic suspension and, after drying, is removed by combustion leaving a porous ceramics. The pore size of the sponge determines the pore size of the final product after firing shrinkage. The foam must have open cells, a uniform degree of porosity, good flexibility, no combustion residue and a good ability to recover its original shape. In the foaming method, a suitable reactant is added to the ceramic suspension to develop a gas phase, which creates bubbles in the material and causes it to foam. The subsequent drying and firing stages lead to the consolidation of the porous structure with the complete burn out of the foaming agent.

The first technique typically generates open-cell structures, while sponges of small pore size and closed porosity cannot be obtained. With the foaming method, it is possible to produce both open- and closed-pore materials having different density, shape and composition.[19] Very porous ceramic materials (lead titanate aerogels with pore volume fraction 86%) have been obtained via a sol-gel process and drying in supercritical carbon dioxide[22] but no piezoelectric properties have been reported in this case.

The other three methods are traditional processes. One of the most common method for making porous ceramic is by powder pressing and sintering; in this way a porous network is formed by the spaces between the necked powders, and the stability of the pores is achieved by controlling the sizes of the particles. The degree of porosity is controlled by the degree of partial sintering, which, in turn, is controlled by sintering at different temperature and/or different times. An alternative way to produce porosity is to mix organic particulate into the powder compact in the powder preparation stage or, in the case of tape casting, into the slurry preparation stage. These organic particulates can be chosen so that they pyrolyze during the binder removal step, leaving stable voids that are not removed during the subsequent sintering procedure.

In the present paper we investigated the effect of polymer volume and properties and sintering temperature on the microstructure of lead zirconate titanate (PZT) porous samples, that ultimately influences their physical properties. A wide range of pore volumes and pore size distribution was obtained following three different preparation procedures: (a) reduction of the sintering temperature of samples prepared by die pressing of the PZT powder, (b) use of a different forming technique like tape casting, starting from slurries with high volume of organic content, (c) addition of two different volume concentrations of organic polymer to the powder and sintering the die pressed samples. To our knowledge this is the first detailed microstructural study on porous piezoelectric ceramics which takes into consideration the role of different parameters in the formation of a definite microstructure and consequently in the final value of physical properties of those materials.

2. Experimental procedure

The samples have been prepared starting from PZT powder with composition $Pb_{0.988}[(Zr_{0.52}Ti_{0.48})_{0.976}Nb_{0.024}]O_3$, calcined at 850°C. It has been found by preliminary studies that calcination at this temperature for 4 h leads to complete perovskite phase formation.[23] The PZT powder is characterised by the following equivalent particle diameter: $d_{10} = 0.8$ μm, $d_{50} = 1.4$ μm, $d_{90} = 2.7$ μm at 10, 50 and 90% cumulative weight, respectively.

A first set of samples (type A) was obtained by uniaxial pressing into pellets at 100 MPa the as calcined powder followed by sintering at 1000°C (sample A00), 1050°C (sample A05) and 1100°C (sample A11) with 30 min of soaking time. Samples type B were prepared by firing at 1000 and 1100°C tape cast material. For this purpose suitable slurries were prepared in an azeotropic mixture of methyl-ethyl-ketone and ethanol, using glycerol tryoleate as deflocculant.

Two binders based on polyvinylbutyral with different average molecular weight (55.000 and 105.000) and a plasticizer (butyl-benzyl-phtalate) were used; the slurry composition and the powder/solvent/deflocculant/binder/plasticizer ratio has been kept constant. The PZT powder was first deagglomerated in the solvent with the deflocculant by ball milling for 1 h in a Teflon jar using zirconia milling media. The first binder was then added and, after a further homogenisation of 1 h, the second binder and plasticizer were added and the ball milling was continued for 20 h. Then the slurry was tape cast onto a mylar support, moving at a constant speed of 20 cm/min, with a laboratory tape casting bench which had a stationary double blade system. The tape was dried at room temperature without air flowing and then stripped from the support. The firing was performed at the heating rate of 20°C/h until 600°C to allow the organic burn out process, and 100°C/h up to the final sintering temperature of 1000°C or 1100°C with 30 min of soaking time.

Samples type C and D were prepared by uniaxial pressing, into pellets, at 100 MPa the as calcined PZT powder previously dry mixed with two different volume fractions, 40 and 50%, respectively, of methyl-hydroxyethyl-cellulose (MHEC). The particle size distribution of the raw MHEC is very broad (1-400 μm) with the mean particle diameter $d_{50} \approx 72$ μm while $d_{10} \approx 10$ μm and $d_{90} \approx 140$ μm. From thermogravimetric analysis the optimum heating cycle was found to consist in an initial heating rate of 100°C/h up to 200°C followed by a rate of 50°C/h up to 450°C to assure the complete burn out

of the organic additive. The heating treatment has been afterwards continued with a rate of 100°C/h up to 600°C and 200°C/h up to the final sintering value which varied in the range 1100–1200°C for C products (samples C10–C20) and in the range 1000–1200°C for D products (samples D00–D20) with 30 min of soaking time.

During sintering all the samples were placed on fired setters in closed high purity alumina crucibles and a small amount of $PbZrO_3$ was added as a source of Pb.

The composition expressed as PZT to binder volume ratio, processing parameters, green and final densities and pore volume of the obtained samples are reported in Table 1. The green density was geometrically measured while the sintered density was obtained from the weight/volume ratio assuming as volume sample the mercury volume displaced by sample in the porosimetric analysis since no macropores were present. The last column of Table 1 represents the pore volume fraction as obtained from mercury porosimetry which does not necessarily coincides with the pore volume fraction calculated from the relative density value. After sintering the samples were electroded on both faces with silver paste and poled at 3 kV/mm for 40 min in a silicone oil bath at 120°C. The physical properties have been measured few days after the poling on samples carefully cleaned with acetone in ultrasonic cleaning bath.

All samples have been analysed by X-ray diffraction, mercury intrusion porosimetry and scanning electron microscopy (SEM). Piezoelectric, dielectric and elastic properties were determined by different techniques like electrical impedance method and interferometric heterodyne technique on samples of standard shapes and dimensions, as recommended by IEEE standards. More details about these properties and the corresponding measurement techniques have been given elsewhere.[10]

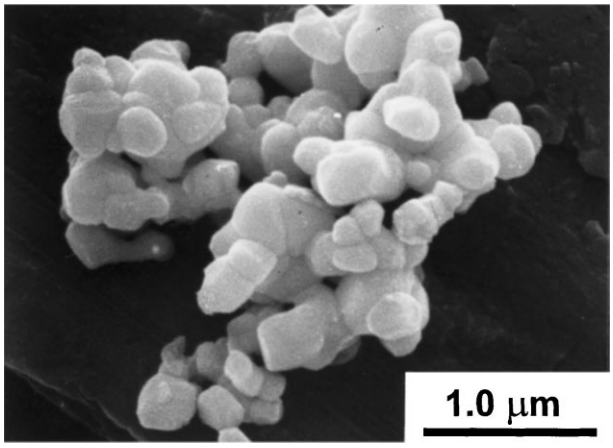

Fig. 1. SEM morphology of the PZT calcined powder.

3. Results and discussion

The SEM micrograph of PZT powder, reported in Fig. 1 shows the presence of aggregates of rounded shape with mean diameter of 1.4 μm in which the primary particles have an average size of about 0.4 μm. The average particle size of powder, measured by X-ray sedimentation technique (Sedigraph, Micromeritics USA), was about 1.4 μm and more than 90% of the particle size ranged from 0.1 to 3.0 μm. This fact would facilitate the sintering of the powder as reported in Ref. 24 and confirm that sedigraph measurements are a good indication of the average agglomerate size rather than average particle size.

The X-ray diffraction spectra of all the porous samples evidenced the presence of both rombohedral and tetragonal phases, with a predominance of rombohedral phase, as shown in Fig. 2

Table 1
Composition, processing parameters and physical characteristics of PZT samples

Sample	PZT/binder (vol.%)	Sintering[a] temperature (°C)	Green density (g cm^{-3})	Sintered density (g cm^{-3})	Rel. sintered density[b] (%)	Linear shrinkage (%)	Pore volume[c] (%)
A10	100/0	1100	4.50	7.45	93.0	15.4	1.8
A05	100/0	1050	4.46	6.66	83.2	12.4	15.2
A00	100/0	1000	4.50	5.31	66.3	6.7	36.2
B10	50/50	1100	3.86	4.50	56.2	–	44.9
B00	50/50	1000	3.86	4.40	55.0	8.6	46.3
C20	60/40	1200	3.48	5.00	62.4	12.6	33.4
C18	60/40	1180	3.50	5.01	62.6	11.7	36.5
C10	60/40	1100	3.54	3.68	46.0	3.7	52.0
D20	50/50	1200	3.27	4.84	60.4	13.4	38.1
D18	50/50	1180	3.22	4.47	55.8	9.3	38.8
D10	50/50	1100	3.22	3.90	48.7	–	53.3
D00	50/50	1000	3.21	3.31	41.3	5.9	59.4

[a] Soaking time, 30 s.
[b] Theoretical density, 8.006 g cm^{-3}.
[c] Pore volume as determined by mercury porosimetry.

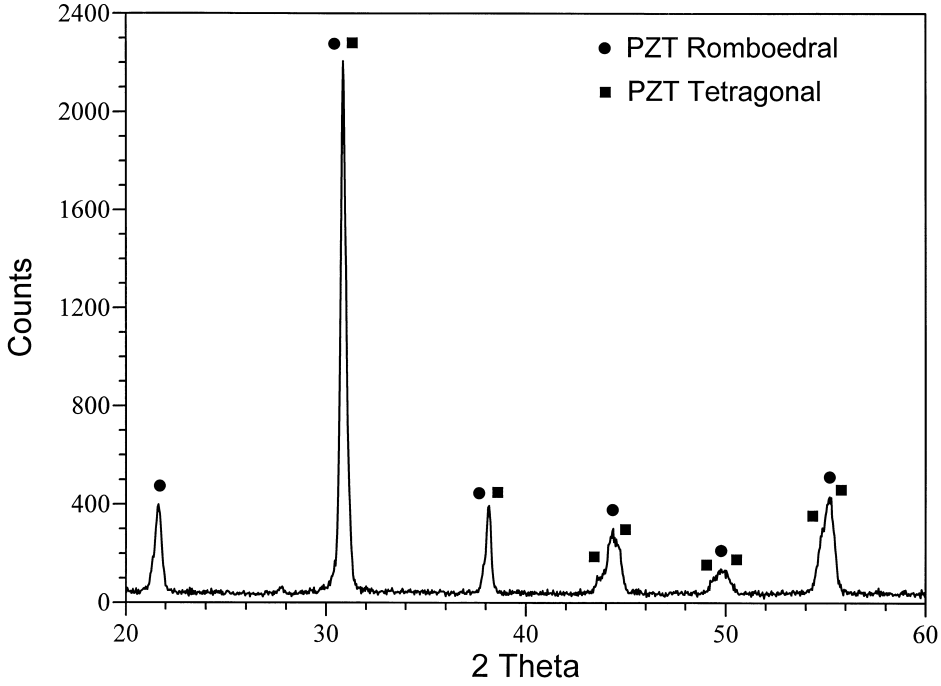

Fig. 2. A typical XRD spectrum of the sintered porous PZT samples.

In this work, we emphasise the influence of some parameters, as sintering temperature and quantity of the additive, on microstructure and pore size distribution. Previously one should mention that interpretation of the data on pore size distribution as measured by mercury porosimetry is not straightforward. Indeed, when referring to pores, these can be divided in at least two groups: "pore bodies" where most porosity resides and "pore throats" which are the channels connecting the first pore bodies. Different models based on percolation theory[16] have been used for interpretation of pressure variation in these experiments and an average pore size diameter is attributed to pores whose volume is equal to that of a cylinder of the same diameter.

Let us examine first the pore size distribution of the type A samples which are obtained by die pressing the calcined powder followed by the heat treatment at a temperature with 100–200°C lower than that generally used to obtain full density PZT ceramics (1200°C). The pore size in the green body before sintering is determined by the packing process of primary particles and agglomerates; the mean relative green density value of 56.1% obtained for A green samples evidence a good packing behaviour of the powder. The pore size distribution of an A green sample, reported in Fig. 3, shows a rather monomodal distribution with about 80% of the pore radius in the range 0.085–0.15 μm. A low sintering temperature (1000°C) allows to obtain a relative sintered density of 66.3% (sample A00) which increases until 93.0% at 1100°C (sample A10) proving the good sinterability of these samples. Very small pore radius and a narrow size distribution is found in the

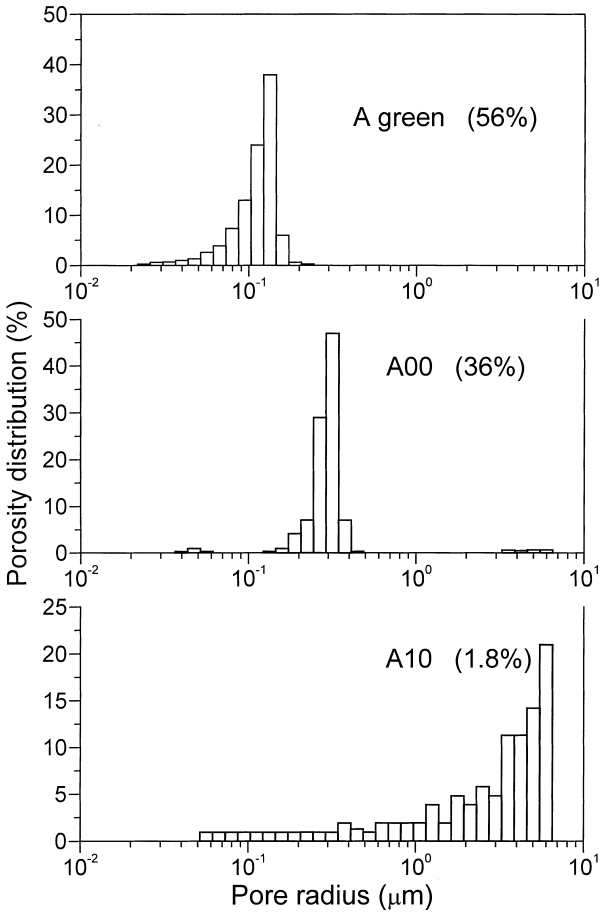

Fig. 3. Pore size distribution for type A samples: A_{green} heat treated at 450°C, A00 sintered at 1000°C, A10 sintered at 1100°C (pore volume is reported in parentheses).

samples A00 and A05, while very few big pores (pore volume 1.8 vol%) with a broad presence of micro and meso porosity, are found in sample A10 (Fig. 3). This small porosity value leads to suppose the presence of a closed porosity formed during sintering process.

Samples type B result from the colloidal processing of the powder which is firstly dispersed in organic solvent by adsorption of glycerol tryoleate; the further addition of soluble polymer binders and plasticizer interconnect powder particles by forming a network of links that provides strength and toughness to the thin sheets obtained by tape casting of the optimised slurry. The resulting cast body, after burn out of the organic additives (sample B green), shows an homogeneous structure, with a relative green density of about 48%. The green morphology is still very homogeneous, the porosity distribution is almost monomodal with a maximum at about 0.3 μm and a spectrum enlarged toward smaller pore widths (Fig. 4); this pore structure is mostly originated from the combustion of the polymeric film covering the well dispersed powder. The sintering at 1000°C produces a reduction of pore volume (46%) with a slight increase of the diameter that roughly doubles upon sintering at 1100°C without any relevant decrease of pore volume (Fig. 4). The degree of powder densification in tape cast samples B is lower than that of the pressed samples A at the same temperature; in particular A10 sample can be considered as quite fully dense product while the B10 sample shows a relative density of 56.2% with a pore volume of about 45%.

Porous samples type C and D are obtained by dry mixing calcined PZT powder with a cellulose derivative with broad particle size distribution which acts as porosity inducing agent. The organic particles can be regarded as inclusions added to the green structure of samples A leading to a relative green density of 44% (porosity 56 vol.%) or 40% (porosity about 60%) of the theoretical value depending on the cellulose volume percentage (40 or 50%). The pore size distribution of C10 sample sintered at 1100°C, together with the low shrinkage and low pore volume reduction (3%) let us presume that, upon pressing, the cellulose granules break up and mix rather homogeneously with PZT powder so as to give rise to a bimodal distribution of the pore size as reported in Fig. 5. The small pores with the average radius of 0.35 μm can be attributed to the

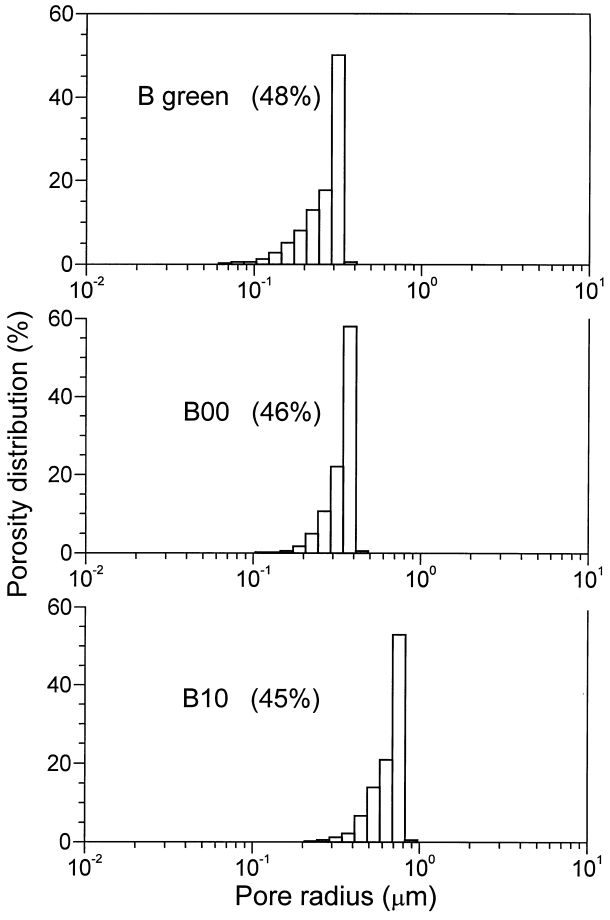

Fig. 4. Pore size distribution for sample type B: B_{green} heat treated at 450°C, B00 sintered at 1000°C, B10 sintered at 1100°C (pore volume is reported in parentheses).

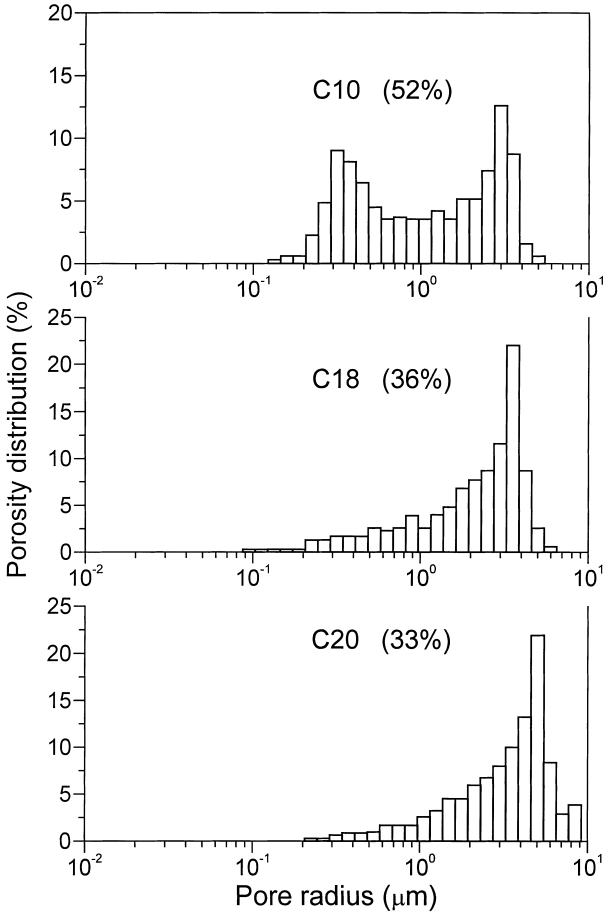

Fig. 5. Pore size distribution for sample type C: C10 sintered at 1100°C, C18 sintered at 1180°C, C20 sintered at 1200°C (pore volume is reported in parentheses).

porosity coming from powders packing process while the pores with the average radius of 3.0 μm are the result of ignition and decomposition reaction of cellulose added as porosity inducing agent. As previously mentioned for the A samples, increasing the sintering temperature the small pores disappear giving rise to a few pores with radius of about one order of magnitude higher. In particular the sample C20, sintered at 1200°C (the temperature at which the powder fully densifies) is still porous with a total pore volume of 33% and the presence of a broadened distribution of large pores with an increased radius dimension until a mean value of 5.0 μm (Fig. 5). The sintering behaviour of D samples is similar to that of C samples although an increased amount of cellulose additive (50 vol.%) is mixed with the PZT powder. For example sample D10 upon sintering at 1100°C shows a pore volume of 53.3%, only 3% higher than that corresponding to C10 sample; large pores with radius of about 3.5 μm prevail, while pores in the whole size range up to 0.2 μm are present. SEM analyses was performed to evaluate the microstructural evolution during heat treatment at different temperatures and the micrographs of fracture surfaces are reported in Fig. 6 and Fig. 7. the morphologies of samples A00 (Fig. 6a) and B00 (Fig. 6b) sintered at 1000°C, are substantially different although the pore size distributions fall in the same range as reported in Figs. 3 and 4; this difference is a consequence of the original presence of organic substance (binders and plasticizer) and their diffusion and flowing out during burn out treatment.

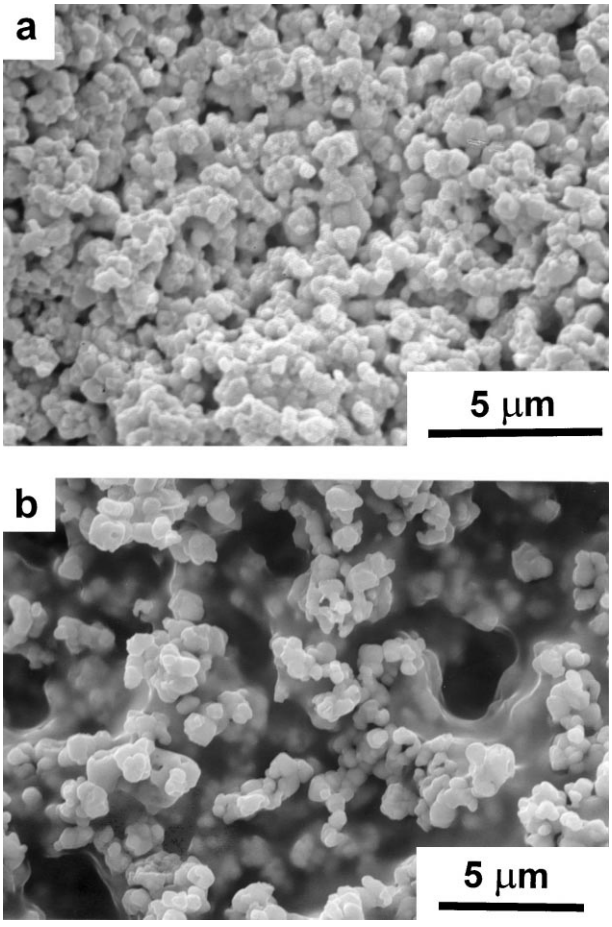

Fig. 6. SEM morphology of (a) sample A00 and (b) sample B00, both sintered at 1000°C.

Sample A, die pressed, shows an homogeneous particle distribution with a quite uniform porosity having a mean value at 0.3 mm. The distance between the particles agglomerate, in the sample B obtained by tape casting, is quite different and bigger than in sample A according with the total porosity of 46% which is with about 20% higher than sample A porosity. The same pore size distribution can be explained with the presence of small bottle-necks between big pores; in the porosimetric analysis the bottle-necks determine the pore radius while the big pores determine the pore volume.

The essentially bimodal distribution of pore size of previously mentioned sample C10 is well evidenced in Fig 7 a and b while the almost fully dense structure permeated by still interconnected channels arising upon sintering at 1200°C is shown in Fig. 7 c and d for the sample C20. The 1200°C sintering temperature is able to close the "structural porosity" while the large pores, induced by organic agent, remain. The big pores show an irregular shape according to non homogeneous morphology of the MHEC added.

The elastic, piezoelectric and dielectric properties of the porous PZT samples were extensively presented and discussed elsewhere.[10,12,17,18] Most representative physical properties of porous samples prepared with different methods are reported in Table 2. In Figs. 8 and 9, the variations of acoustical impedance $Z = \rho v$ (v = elastic wave velocity), relative dielectric constant ε_r and elastic compliance s_{11}^E with the pore volume fraction are represented. They show an almost regular dependence and their increasing (or decreasing) with porosity can be qualitatively explained by considering the gradual introduction of air filled pores (low dielectric constant and high compliance) in the ceramic matrix (different models based on effective medium theory[25] and percolation theory[9,17] have been used to quantify this dependence in the low and high porosity range, respectively, their applicability to our samples being discussed elsewhere[10,17,18]). Although a definite trend can be identified in Figs. 8 and 9, a certain dispersion of the results is also observed, which is certainly due to their different pore size distribution. For example, samples A00 and C18 have almost the same pore volume fraction (about 36%) but very different acoustical impedance values [13 and 9.2×10^6 kg/(m^2 s), respectively], as well as very different relative dielectric constant values (500 and 241, respectively); these physical properties differences should be nevertheless attributed to their very dissimilar pore size distribution, which is narrow (with a mean

radius of about 0.3 μm) for sample A00 (Fig. 3) and very broad (ranging between 0.1 and 6 μm, with a mean size of about 3 μm) for sample C18 (Fig. 5). But, as can be seen from Table 2, differences in pore size distribution most dramatically affect the mechanical quality factor Q_m as well as those constants which couple mechanical variables to electrical variables such as piezoelectric constants and electromechanical coupling factors. Fig. 10 illustrates this discussion for the case of Q_m. Mechanical quality factor is inversely proportional

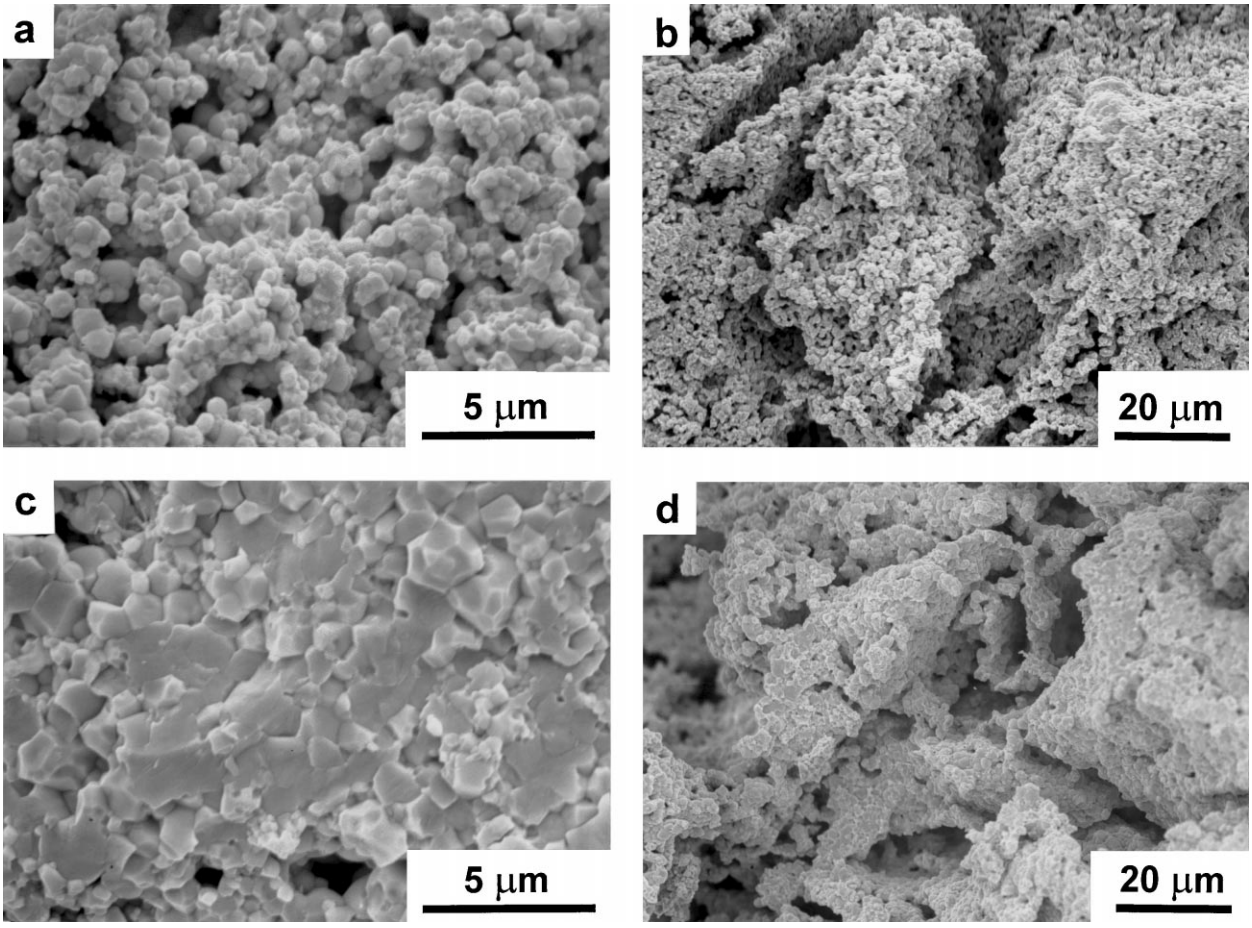

Fig. 7. SEM morphology of (a) and (b) sample C10 sintered at 1100°C and (c) and (d) sampe C20 sintered at 1200°C.

Table 2
Elastic, piezoelectric and dielectric properties of the porous samples

Sample	σ_p	$\varepsilon_{33}/\varepsilon_p$	k_p	$-k_{31}$	s_{11}^E	$-d_{31}$	d_{33}	$-g_{31}$	g_{33}	$d_h g_h$	V_{tr}	Z	Y_{11}	Q_m
					(10^{-12} m^2/N)	(10^{-12} m/V)		(10^{-3} Vm/N)		(10^{-15} m^2/N)	(m/s)	(10^6 kg/m^2 s)	(10^{10} N/m^2)	
A10	0.45	1290	0.57	0.30	18.59	136.8	–	12.0	–	–	2684	20.0	5.37	90.1
A05	0.38	671	0.19	0.11	21.06	37.4	100.0	6.3	16.8	106	2669	17.0	4.74	41.8
A00	0.33	500	0.22	0.13	32.02	49.0	120.0	11.0	27.1	112	2376	13.0	3.12	55.7
B10	0.30	190	0.20	0.12	74.10	46.2	115.6	21.3	68.7	320	1814	7.4	1.35	36.5
B00	0.34	192	0.16	0.09	60.70	29.0	–	15.1	–	–	1931	8.6	1.65	50.4
C18	0.26	241	0.16	0.10	54.20	33.8	89.7	15.8	41.9	230	1941	9.2	1.80	45.0
C10	0.30	62	0.13	0.08	162.00	22.5	97.4	40.8	91.1	500	1309	4.7	0.62	72.0
D18	0.30	72	0.15	0.09	134.00	26.1	142.3	41.1	–	–	1345	5.5	0.75	60.1
D10	0.37	160	0.20	0.11	100.80	40.1	93.5	28.3	66.0	125	1535	6.4	0.99	36.8

to mechanical loss whose microscopic origin, in a ferroelectric material such as PZT, resides in the movement of ferroelectric domain walls driven by an external field. In order to try a qualitative explanation of the influence of pore size distribution on Q_m, in Fig. 10 we have identified and marked three couples of samples corresponding to almost the same porosity values, but presenting different pore size distributions. These are: A00–C18 (porosity 36%), B00–B10 (porosity ~ 45%) and C10-D10 (porosity ~ 53%). In all three couples samples with higher Q_m show either a narrow pore size distribution with small pores (samples A00 and B00) or an appreciable quantity of small pores (sample C10); instead the samples with lower Q_m have either a broad pore size distribution formed mainly by large pores, with radius of a few micrometers, like C18 and D10 (sample D10, not shown in Figs. 3–5, has a broad size distribution with a prevalence of large pores with radius of about 3.5 μm, as previously mentioned), or a narrow size distribution but with larger pores as sample B10 where the radius is about 0.7 μm (almost double if compared with B00). In few words, the idea is that a sample with a certain porosity shows a higher total pore surface if its porosity is formed by small pores than if it would be formed by large pores. As pore surface might restrict the movement of ferroelectric domain walls (domain pinning), a low mechanical vibration loss and hence a high Q_m is obtained in samples with a higher total pore surface, at a given porosity value.

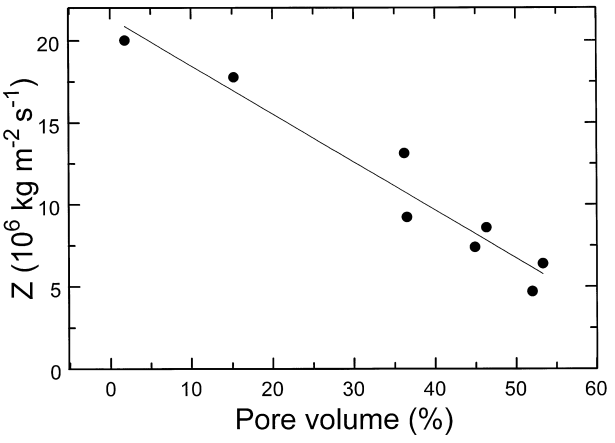

Fig. 8. Acoustic impedance as a function of pore volume fraction.

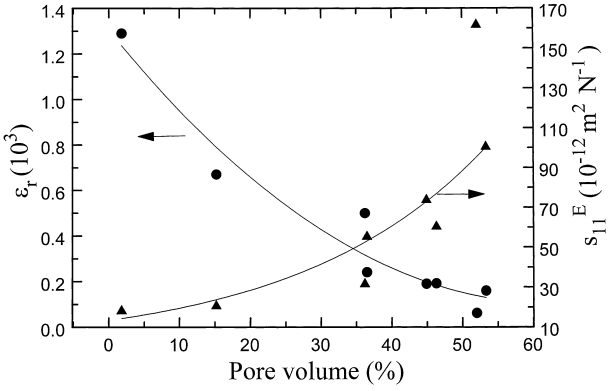

Fig. 9. Dielectric permittivity and elastic compliance as a function of pore volume fraction.

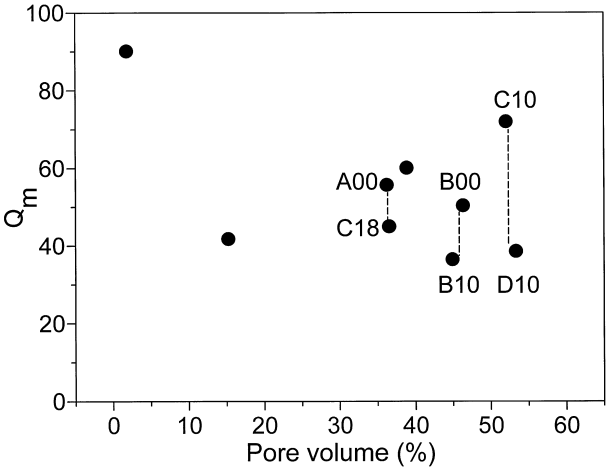

Fig. 10. Mechanical quality factor Q_m versus pore volume fraction.

Our results make it quite clear that fabricating porous piezoelectric samples with reproducible properties is a difficult task, since samples with the same porosity fraction but obtained with various methods present very different microstructures and consequently very different properties. Moreover, the absence of a valid model for the dependence of piezoelectric properties on pore size distribution is a further difficulty. We hope that our results could represent a stimulus for the construction of a realistic model.

4. Conclusions

In conclusion, we have shown that physical properties dispersion previously observed in porous samples could be attributed to differences introduced by various preparation methods. Pore size distribution and microstructural differences resulting from various processing parameters influence physical properties and careful microstructural design and preparation procedure has to be adopted if reproducible results must be obtained, in the range of high and medium porosity values.

References

1. Hikita, K., Yamada, K., Nishioka, M. and Ono, M., Piezoelectric properties of the porous PZT and porous PZT composite with silicone rubber. *Ferroelectrics*, 1983, **49**, 265–272.
2. Ting, R. Y., Piezoelectric properties of a porous PZT ceramic. *Ferroelectrics*, 1985, **65**, 11–20.
3. Bast, U. and Wersing, W., The influence of internal voids with 3-1 connectivity on the properties of piezoelectric ceramics prepared by a new planar process. *Ferroelectrics*, 1989, **94**, 229–242.

4. Matsunaka T., Tabuchi Y., Kasai C., Tachikawa K., Kyono H. and Ikeda H., In *Proceeding Ultrasonics Symposium*, 1988, pp. 681–684.
5. Hayashi, T., Sugihara, S. and Okazaki, K., Processing of porous 3-3 PZT ceramics using capsule-free O_2–HIP. *Jpn J. Appl. Phys.*, 1991, **30**(9B), 2243–2246.
6. Arai, T., Ayusawa, K., Sato, H., Miyata, T., Kawamura, K. and Kobayashi, K., Properties of Hydrophone with Porous Piezoelectric Ceramics. *Jpn J. Appl. Phys.*, 1991, **30**(9B), 2253–2255.
7. Mizumura, K., Kurihara, Y., Ohashi, H., Kumamoto, S. and Okuno, K., Porous piezoelectric ceramic transducer. *Jpn J. Appl. Phys.*, 1991, **39**(9B), 2271–2273.
8. Kumamoto, S., Mizumura, K., Kurihara, Y., Ohhashi, H. and Okuno, K., Experimental evaluation of cylindrical ceramic tubes composed of porous Pb(Zr Ti)O_3 ceramics. *Jpn J. Appl. Phys.*, 1991, **30**(9B), 2292–2294.
9. Gaillard-Groleas, C., Lagier, M. and Sornette, D., Critical behaviour in piezoelectric ceramics. *Phys. Rev. Lett.*, 1990, **64**, 1577–1580.
10. Craciun, F., Galassi, C., Roncari, E., Filippi, A. and Guidarelli, G., Electro-elastic properties of porous piezoelectric ceramics obtained by tape casting. *Ferroelectrics*, 1998, **205**, 49–67.
11. Roncari E., Galassi C., Craciun F., Guidarelli G., Marselli S. and Pavia V., Ferroelectric ceramics with included porosity for hydrophone applications. In *Proc. of the 11th IEEE International Symposium on Applications of Ferroelectrics ISAF XI*, Montreux, Switzerland, 1998, pp. 373–376.
12. Craciun F., Galassi C., Roncari E., Capiani C. and Guidarelli G., Preparation and characterisation of porous piezoelectric ceramics with different porosities. In *Ceramics: Getting into the 2000's, Part E, Advances in science and Technology 17, Proceedings of CIMTEC'98*, ed. P. Vincenzini, Firenze 14–16 June 1998, Techna Srl Pub., 1999, pp. 337–340.
13. Marselli, S., Pavia, V., Galassi, C., Roncari, E., Craciun, F. and Guidarelli, G., Porous piezoelectric ceramic hydrophone. *J. Acoust. Soc. Am.*, 1999, **106**, 733–738.
14. Stauffer, D. and Aharony, A., *Introduction to Percolation Theory*. Taylor and Francis, London, 1992.
15. Havlin S. and Bunde A., Percolation I. In *Fractals and Disordered Systems*, ed. S. Havlin and A. Bunde. Springer-Verlag, Heidelberg, 1991.
16. Sahimi, M., *Applications of Percolation Theory*. Taylor and Francis, London, 1994.
17. Craciun, F., Galassi, C. and Roncari, E., Experimental evidence for similar critical behaviour of elastic modulus and electric conductivity in porous ceramic materials. *Europhys. Lett.*, 1998, **41**, 55–60.
18. Craciun F., Guidarelli G., Galassi C. and Roncari E., Critical behaviour of ultrasonic wave velocities in porous piezoelectric ceramics. In *Proceedings IEEE Ultrasonics Symposium, IEEE*, New York, 1997, pp. 573–576.
19. Saggio-Woyansky, J., Scott, C. E. and Minnear, W. P., Processing of porous ceramics. *Am. Ceram. Soc. Bull.*, 1992, **71**(11), 1674–1682.
20. Dean-Mo Liu, Fabrication of hydroxyapatite ceramic with controlled porosity. *J. Mater. Sci. Mater. Med.*, 1997, **8**, 227–232.
21. Pugh, R. J., Dispersion and stability of ceramic powders in liquid. *Surfactant Science Vol. 51. Surface and Colloidal Chemistry in Advanced Ceramic Processing*, ed. R. J. Pugh and L. Bergstrom. Markel Dekker Inc, New York, 1992, pp.1674–1682.
22. Loebmann, P. and Glaubitt, W., Densification and crystallisation of lead titanate aerogels. *J. Am. Ceram. Soc.*, 1997, **80**, 2658–2666.
23. Galassi, C., Roncari, E., Capiani, C. and Costa, A., Influence of processing parameters on the properties of PZT materials. In *Piezoelectric Materials: Advances in Science, Technology and Applications*, ed. C. Galassi, M. Dinescu, K. Uchino and M. Sayer. NATO Science Series 3 High Technology, vol. 76, Kluwer Academic Pub, Dordrecht, 1999.
24. Erring, C., *J. Appl. Phys.*, 1950, **21**, 31.
25. Dunn, M. L. and Taya, M., Electromechanical properties of porous piezoelectric ceramics. *J. Am. Ceram. Soc.*, 1993, **76**, 1697–1706.